

## Interhalogen Compounds

Preparation of Two Quantum-Chemically Predicted, Isomeric  $[\text{Br}_4\text{F}_{13}]^-$  Anions in the Solid StateJascha Bandemehr,<sup>[a]</sup> Sergei I. Ivlev,<sup>[a]</sup> Antti J. Karttunen,<sup>[b]</sup> and Florian Kraus\*<sup>[a]</sup>

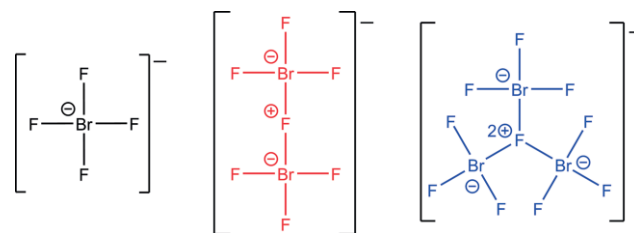
**Abstract:** Two isomeric tridecafluoridotetrabromate(III) anions,  $[\text{Br}_4\text{F}_{13}]^-$ , both previously predicted by quantum-chemical calculations, have serendipitously been obtained from the reaction of  $\text{BrF}_3$  with  $\text{BaF}_2$ . Single crystals of  $\text{Ba}_2[\text{Br}_3\text{F}_{10}]_2[\text{Br}_4\text{F}_{13}]_2$  were selected from the reaction mixture at approximately 10 °C. The crystal structure contains two novel, isomeric  $[\text{Br}_4\text{F}_{13}]^-$  anions besides the known, star-shaped  $[\text{Br}_3\text{F}_{10}]^-$  anions. It crystallized in the monoclinic space group  $P1n1$  (No. 7) with  $a = 8.8519(18)$ ,  $b = 15.217(3)$ ,  $c = 14.628(3)$  Å,  $\beta = 90.34(3)^\circ$ ,  $V = 1970.4(7)$  Å<sup>3</sup> and  $Z = 2$ ,  $mP124$  at 100 K. The compound was additionally

investigated using quantum-chemical solid-state calculations. If however crystals from the above reaction mixture were selected at room temperature, the compound  $\text{Ba}[\text{Br}_3\text{F}_{10}]_2 \cdot \text{BrF}_3$  was obtained containing disordered  $\text{BrF}_3$  molecules of crystallization besides  $[\text{Br}_3\text{F}_{10}]^-$  anions. The  $[\text{Br}_4\text{F}_{13}]^-$  molecules were no longer present.  $\text{Ba}[\text{Br}_3\text{F}_{10}]_2 \cdot \text{BrF}_3$  crystallized in the cubic space group  $Pa\bar{3}$  (No. 205) with  $a = 12.4903(14)$  Å,  $V = 1948.6(7)$  Å<sup>3</sup>,  $Z = 4$ ,  $cP124$ ,  $T = 100$  K. The much easier to handle latter compound was additionally investigated using powder X-ray diffraction, as well as IR and Raman spectroscopy.

## Introduction

Compounds containing fluoridobromate(III) anions are powerful oxidizers and fluorinating agents.<sup>[1]</sup> Up to now, three structurally different fluoridobromate(III) anions are known, containing one, two or three bromine atoms, that is, mono-, bi- and trinuclear anions, if the Br atoms are considered as central atoms. The first reported anion of this kind was the mononuclear tetrafluoridobromate(III) anion  $[\text{BrF}_4]^-$ . Such square-planar anions are contained in the compounds  $A[\text{BrF}_4]$  ( $A = \text{Na}$ ,<sup>[2–4]</sup>  $\text{K}$ ,<sup>[1,3–11]</sup>  $\text{Rb}$ ,<sup>[3,4,12–14]</sup>  $\text{Cs}$ ,<sup>[10,15,16]</sup>  $\text{Ag}$ ,<sup>[1,17]</sup>  $\text{NO}$ ,<sup>[10]</sup>  $\text{NO}_2$ ,<sup>[10]</sup>  $\text{NF}_4$ ,<sup>[18]</sup>  $\text{NMe}_4$ ,<sup>[19]</sup>) and  $\text{Ba}[\text{BrF}_4]_2$ .<sup>[1,20]</sup> The bi- and trinuclear anions were synthesized by Lewis acid-base reactions of  $[\text{BrF}_4]^-$  anions with  $\text{BrF}_3$  and have only recently been identified and their structures elucidated. The binuclear heptafluoridodibromate(III) anion  $[\text{F}_3\text{Br}-(\mu\text{-F})-\text{BrF}_3]^-$  is known for the compounds  $A[\text{Br}_2\text{F}_7]$ <sup>[21]</sup> ( $A = \text{Rb}$ ,<sup>[22]</sup>  $\text{Cs}$ <sup>[15,23]</sup>),  $\text{PbF}[\text{Br}_2\text{F}_7]$ <sup>[24]</sup> and the trinuclear decafluoridotribromate(III) anion  $[(\mu_3\text{-F})(\text{BrF}_3)_3]^-$  so far only for the compounds  $A[\text{Br}_3\text{F}_{10}]$  ( $A = \text{Rb}$ ,  $\text{Cs}$ ).<sup>[21,22]</sup> The structural formulas

of the currently known anionic species are shown in Scheme 1, stereochemical aspects are not considered for simplicity.



Scheme 1. Structural formulas of currently known fluoridobromate(III) anions. The  $[\text{BrF}_4]^-$  anion is shown in green, the  $[\text{Br}_2\text{F}_7]^-$  anion in red, and the  $[\text{Br}_3\text{F}_{10}]^-$  anion in blue.

The  $[\text{BrF}_4]^-$  and  $[\text{Br}_2\text{F}_7]^-$  anions are isostructural to the corresponding fluoroaurate(III) anions  $[\text{AuF}_4]^-$  and  $[\text{Au}_2\text{F}_7]^-$ .<sup>[9,25]</sup> To the best of our knowledge, the trinuclear anion  $[(\mu_3\text{-F})(\text{AuF}_3)]^-$  is still unknown. Tetranuclear tridecafluoridotetrabromate(III) anions,  $[\text{Br}_4\text{F}_{13}]^-$ , have previously been predicted by us based on quantum-chemical calculations for the gas phase (Scheme 2),<sup>[26]</sup> and the chain-like isomer shown in Scheme 2a was of lowest energy, while those of Scheme 2b and Scheme 2c were only 7 and 3 kJ/mol higher in Gibbs free energy, respectively.

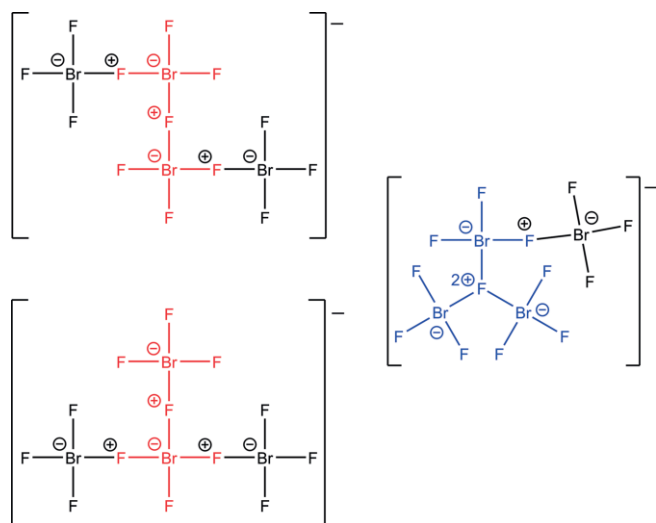
We serendipitously obtained the  $[\text{Br}_4\text{F}_{13}]^-$  anions shown in Scheme 2b and Scheme 2c when trying to synthesize  $\text{Ba}[\text{BrF}_4]_2$ : As the crystal structure of  $\text{Ba}[\text{BrF}_4]_2$  was derived from powder X-ray diffraction data,<sup>[20]</sup> we tried to obtain single-crystals of the compound by adding  $\text{BrF}_3$  to  $\text{BaF}_2$  or  $\text{BaCl}_2$ . Instead of  $\text{Ba}[\text{BrF}_4]_2$  we first obtained a compound containing  $[\text{Br}_3\text{F}_{10}]^-$  anions and  $\text{BrF}_3$  molecules of crystallization, but then a phase change to a compound with two isomeric  $[\text{Br}_4\text{F}_{13}]^-$  anions seemed to have occurred.

[a] J. Bandemehr, Dr. S. I. Ivlev, Prof. Dr. F. Kraus  
Fachbereich Chemie, Philipps-Universität Marburg,  
Hans-Meerwein-Str. 4, 35032 Marburg, Germany  
E-mail: f.kraus@uni-marburg.de

[b] Prof. Dr. A. J. Karttunen  
Department of Chemistry and Materials Science, Aalto University,  
00076 Aalto, Finland

Supporting information and ORCID(s) from the author(s) for this article are available on the WWW under <https://doi.org/10.1002/ejic.202000875>.

© 2020 The Authors. European Journal of Inorganic Chemistry published by Wiley-VCH GmbH. This is an open access article under the terms of the Creative Commons Attribution License, which permits use, distribution and reproduction in any medium, provided the original work is properly cited.



Scheme 2. Quantum-chemically predicted  $[\text{Br}_4\text{F}_{13}]^-$  isomers of lowest energy for the gas phase. a) a chain-like  $[\text{Br}_4\text{F}_{13}]^-$  anion that can be rationalized with a central  $[\text{Br}_2\text{F}_7]^-$  anion in red and two attached  $\text{BrF}_3$  molecules, b) a branched isomer with a central  $[\text{Br}_2\text{F}_7]^-$  anion in red and two attached  $\text{BrF}_3$  molecules, and c) a  $[\text{Br}_3\text{F}_{10}]^-$  anion in blue with a  $\text{BrF}_3$  molecule attached.

## Results and Discussion

Adding  $\text{BrF}_3$  to either  $\text{BaF}_2$  or  $\text{BaCl}_2$  at room temperature resulted in an orange suspension forming an orange solution after heating to 80–120 °C. Upon cooling to room temperature, the growth of a few colorless crystals from the solution was observed. The very reactive crystals decomposed during the crystal selection upon contact with the dry glass of the microscope slide. They were handled using polymer loops for mounting, however, these loops sometimes caught fire upon contact with the crystals. This of course led also to the decomposition of the crystals. Despite these problems we were able to mount a single-crystal on the goniometer head of the X-ray diffractometer and determine a cubic unit cell. The crystal structure contained the known  $[\text{Br}_3\text{F}_{10}]^-$  anion and some disordered  $\text{BrF}_3$  molecules, and the composition  $\text{Ba}[\text{Br}_3\text{F}_{10}]_2 \cdot \text{BrF}_3$  was determined. The composition of the bulk phase has been determined by Rietveld refinement, see below.

### Crystal Structure of Cubic $\text{Ba}[\text{Br}_3\text{F}_{10}]_2 \cdot \text{BrF}_3$

Crystals that were selected at room temperature and rapidly chilled to 100 K belonged to the cubic crystal system, space group  $Pa\bar{3}$  (No. 205), with lattice parameter  $a = 12.4903(14)$  Å,  $V = 1948.6(7)$  Å<sup>3</sup>,  $Z = 4$ . Table S1 contains selected crystallographic data and details of the structure determination, Table S2 and Table S3 list atom positions, equivalent isotropic and anisotropic displacement parameters. Only the positions of the

barium atoms and of the atoms of the  $[\text{Br}_3\text{F}_{10}]^-$  anions could be refined, whereas the  $\text{BrF}_3$  molecules of crystallization showed severe disorder and therefore were removed by the squeeze procedure. According to the squeeze routine in Platon,<sup>[27]</sup> the voids, which correspond to the positions of the disordered  $\text{BrF}_3$  molecules, have a volume of circa 75 Å<sup>3</sup>. This is only a bit larger than the volume of 64 Å<sup>3</sup> of a  $\text{BrF}_3$  molecule.<sup>[28]</sup> An estimated unit cell volume for a compound with the composition  $\text{Ba}[\text{Br}_3\text{F}_{10}]_2$  with  $Z = 4$  would be circa 1772 Å<sup>3</sup> when a volume of 59 Å<sup>3</sup> for  $\text{BaF}_2$  (at room temperature) is used. With four more  $\text{BrF}_3$  molecules of crystallization the estimated unit cell volume rises to 2028 Å<sup>3</sup>, which is in good agreement with the 1948.6(7) Å<sup>3</sup> observed by us. According to this consideration, which allows us to estimate the content of  $\text{BrF}_3$  molecules of crystallization, we give the formula of the compound as  $\text{Ba}[\text{Br}_3\text{F}_{10}]_2 \cdot \text{BrF}_3$ . The number of electrons determined by the squeeze procedure is with 37 smaller than the expected 62 for  $\text{BrF}_3$  which would lead to the composition  $\text{Ba}[\text{Br}_3\text{F}_{10}]_2 \cdot 0.6\text{BrF}_3$ . For simplicity, we will use  $\text{Ba}[\text{Br}_3\text{F}_{10}]_2 \cdot \text{BrF}_3$ .

The structure of the  $[\text{Br}_3\text{F}_{10}]^-$  anion contained in this compound is comparable to the previously reported ones in  $A[\text{Br}_3\text{F}_{10}]$  ( $A = \text{Rb}, \text{Cs}$ ) and shown in Figure 1.<sup>[22]</sup>

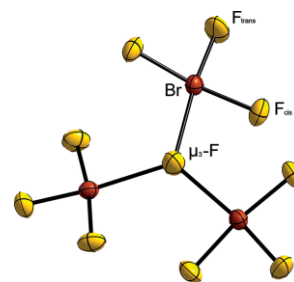


Figure 1. The  $[\text{Br}_3\text{F}_{10}]^-$  anion of the compound  $\text{Ba}[\text{Br}_3\text{F}_{10}]_2 \cdot \text{BrF}_3$ . Displacement ellipsoids shown at 70 % level at 100 K.

The Br–F bond lengths and a comparison to the previously reported ones are listed in Table 1.<sup>[22]</sup> As can be seen from the table the respective Br–F distances are in similar ranges among the compounds. It should be noted that the atom positions and therefore also the atom distances within  $\text{Ba}[\text{Br}_3\text{F}_{10}]_2 \cdot \text{BrF}_3$  are biased due to the squeeze treatment of the disordered  $\text{BrF}_3$  molecules of crystallization, however the magnitude of this influence on the numbers is unknown to us.

The longest Br–F bond lengths are observed for those of the  $\mu_3$ -bridging F atom to the coordinating Br atoms and the shortest for the F atoms which are in *trans* position to the  $\mu_3$ -bridging one, called  $F_{\text{trans}}$ , as it was also the case in  $A[\text{Br}_3\text{F}_{10}]$  ( $A = \text{Rb}, \text{Cs}$ ).<sup>[22]</sup> The  $\mu_3\text{-F-Br-F}_{\text{cis}}$  angles are 86.91(12)° and 101.06(11)°, and the  $\mu_3\text{-F-Br-F}_{\text{trans}}$  angle is 173.33(13)°. Almost-planar, kite-like  $\text{BrF}_4$ -units that are similar to those of the previously described  $[\text{Br}_3\text{F}_{10}]^-$  anions, are present.<sup>[22]</sup> The fluorine

Table 1. A comparison of Br–F bond lengths (in Å) in the  $[\text{Br}_3\text{F}_{10}]^-$  anions for  $\text{Ba}[\text{Br}_3\text{F}_{10}]_2 \cdot \text{BrF}_3$ ,  $\text{Ba}_2[\text{Br}_3\text{F}_{10}]_2[\text{Br}_4\text{F}_{13}]_2$ , and  $A[\text{Br}_3\text{F}_{10}]$  ( $A = \text{Rb}, \text{Cs}$ ).

	$\text{Ba}[\text{Br}_3\text{F}_{10}]_2 \cdot \text{BrF}_3$	$\text{Ba}_2[\text{Br}_3\text{F}_{10}]_2[\text{Br}_4\text{F}_{13}]_2$	$\text{Rb}[\text{Br}_3\text{F}_{10}]^{[22]}$	$\text{Cs}[\text{Br}_3\text{F}_{10}]^{[22]}$
Br– $F_{\text{trans}}$	1.723(3)	1.726(6)–1.744(6)	1.745(2)–1.752(2)	1.746(6)–1.767(7)
Br– $F_{\text{cis}}$	1.847(3), 1.853(3)	1.835(6)–1.874(7)	1.837(2)–1.874(2)	1.824(10)–1.878(7)
Br– $\mu_3\text{-F}$	2.3093(6)	2.243(6)– 2.339(6)	2.243(3)–2.320(3)	2.238(10)–2.329(10)

atoms around the Ba cation are arranged in an icosahedron-like fashion and the Ba–F distances are with 2.746(3) and 2.861(3) Å in good accordance to those of structures with similar coordination polyhedra, for example 2.830(3)–2.855(2) Å in Ba(H<sub>3</sub>F<sub>4</sub>)<sub>2</sub>.<sup>[29]</sup> The Ba atoms are cuboctahedrally surrounded by other Ba atoms and thus are arranged according to the cubic close packing motif. The centers of the tetrahedral voids of the cubic close packing are surrounded by [Br<sub>3</sub>F<sub>10</sub>]<sup>−</sup> anions which are arranged along the edges and the faces of the virtual tetrahedron. The disordered BrF<sub>3</sub> molecules reside within the octahedral voids of the packing. Thus, they are also cubic close packed and the packing of Ba atoms and disordered BrF<sub>3</sub> molecules is in analogy to the NaCl structure type. The crystal structure is shown in Figure 2.

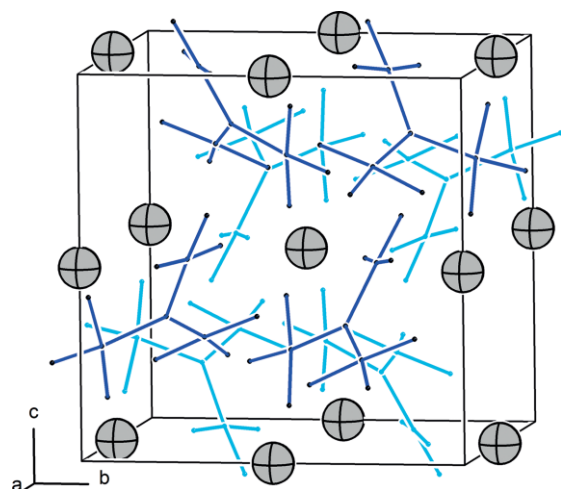


Figure 2. The crystal structure of Ba<sub>2</sub>[Br<sub>3</sub>F<sub>10</sub>]<sub>2</sub>·BrF<sub>3</sub>. Ba atoms are shown in grey with arbitrary radii, wire formulas are shown for the [Br<sub>3</sub>F<sub>10</sub>]<sup>−</sup> anions for the sake of clarity. Those closer to the viewer are drawn in blue, those farther away in pale blue. The voids that are occupied by the BrF<sub>3</sub> molecules of crystallization reside on the corners and the face centers of the unit cell.

During the selection of suitable single crystals for the diffraction experiment on this compound we observed their quite rapid decomposition. It was likely due to hydrolysis from moisture that diffused into the predried perfluorinated oil as no protecting stream of N<sub>2</sub> was used. Therefore, we lowered the temperature of the perfluorinated oil surrounding the crystals to approximately 10 °C, as the melting point of BrF<sub>3</sub> is at 8.8 °C,<sup>[30]</sup> and used a precooled and dried N<sub>2</sub> stream for further protection. Unexpectedly, a phase change seems to have taken place

since the diffraction experiment led to a monoclinic crystal structure for which the unit cell volume was still similar to the one reported above for Ba[Br<sub>3</sub>F<sub>10</sub>]<sub>2</sub>·BrF<sub>3</sub>. Besides the monoclinic ones, we still found some of the cubic crystals described above, so the phase change seems to be not very fast.

### Crystal Structure of Monoclinic Ba<sub>2</sub>[Br<sub>3</sub>F<sub>10</sub>]<sub>2</sub>[Br<sub>4</sub>F<sub>13</sub>]<sub>2</sub>

Table S4 contains selected crystallographic data and details of the structure determination, Tables S5 and S6 hold atom positions, equivalent isotropic and anisotropic displacement parameters of Ba<sub>2</sub>[Br<sub>3</sub>F<sub>10</sub>]<sub>2</sub>[Br<sub>4</sub>F<sub>13</sub>]<sub>2</sub>. The compound crystallizes in space group *P1n1* (No. 7) with *a* = 8.8519(18), *b* = 15.217(3), *c* = 14.628(3) Å, β = 90.34(3)°, *V* = 1970.4(7) Å<sup>3</sup> and *Z* = 2, *mp*124, at 100 K.

We propose that the formation of the monoclinic compound can be described according to Equation (1).



Cooling from room temperature to circa 10 °C seems to be responsible for the phase transformation, in which the disordered BrF<sub>3</sub> molecules of crystallization of the cubic phase become bound to the [Br<sub>3</sub>F<sub>10</sub>]<sup>−</sup> anions.

Two symmetry independent [Br<sub>3</sub>F<sub>10</sub>]<sup>−</sup> anions are present in the crystal structure. The Br–F bond lengths in these [Br<sub>3</sub>F<sub>10</sub>]<sup>−</sup> anions are comparable to those of the previously reported compounds A[Br<sub>3</sub>F<sub>10</sub>] (A = Rb, Cs)<sup>[22]</sup> and are listed in Table 1. Also, the μ<sub>3</sub>–F–Br–F<sub>cis/trans</sub> angles of the almost planar, kite-like BrF<sub>4</sub>–units are similar with 84.1(2)–102.5(3)° and 171.6(3)–177.4(2)° to the previously reported compounds.<sup>[22]</sup> Besides the [Br<sub>3</sub>F<sub>10</sub>]<sup>−</sup> anions, two structurally different [Br<sub>4</sub>F<sub>13</sub>]<sup>−</sup> anions are present. One can be described as a [Br<sub>3</sub>F<sub>10</sub>]<sup>−</sup> anion with an additional BrF<sub>3</sub> molecule connected to an F<sub>cis</sub> atom (see Figure 3).

That *cis* connection is preferred over *trans* connection was previously predicted by us.<sup>[26]</sup> The Br–F bond lengths of this [Br<sub>4</sub>F<sub>13</sub>]<sup>−</sup> anion are listed in Table 2.

The bond length of the μ<sub>3</sub>–bridged F atom to the Br(3) atom, which is also connected to the μ<sub>2</sub>–bridged F(7)<sub>cis</sub> atom, is significantly shorter than the other μ<sub>3</sub>–F–Br(1,2) distances. These two μ<sub>3</sub>–F–Br(1,2) bond lengths are in the same range as for the [Br<sub>3</sub>F<sub>10</sub>]<sup>−</sup> anions. The Br(3)–μ<sub>2</sub>–F(7) bond is, as expected, slightly shorter than the Br(3)–μ<sub>3</sub>–F(4) bond as the latter F atom has a higher coordination number. The shortest Br–F bond lengths in the [Br<sub>4</sub>F<sub>13</sub>]<sup>−</sup> anions are in *trans* position to the μ<sub>2</sub>– and μ<sub>3</sub>–bridg-

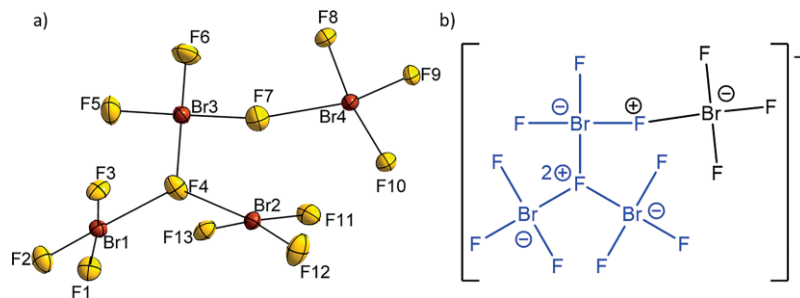


Figure 3. (a) One of the [Br<sub>4</sub>F<sub>13</sub>]<sup>−</sup> anions in the crystal structure of Ba<sub>2</sub>[Br<sub>3</sub>F<sub>10</sub>]<sub>2</sub>[Br<sub>4</sub>F<sub>13</sub>]<sub>2</sub>. Displacement ellipsoids are shown at the 70 % probability level at 100 K. (b) Structural formula of the [Br<sub>4</sub>F<sub>13</sub>]<sup>−</sup> isomer given for direct comparison.

Table 2. Selected Br–F bond lengths (in Å) of the  $[\text{Br}_4\text{F}_{13}]^-$  anion shown in Figure 3.

		observed	calculated DFT-PBE0/def2-TZVP <sup>[26,31]</sup>
$\text{Br}_3\text{F}_{10}$ -unit	Br(1, 2)– $\mu_3$ -F(4)	2.312(6), 2.357(6)	2.39, 2.40
	Br(1)–F(1, 2, 3)	1.859(6), 1.724(6), 1.866(6)	1.84, 1.75, 1.84
	Br(2)–F(11, 12, 13)	1.864(7), 1.737(6), 1.833(6)	1.84, 1.75, 1.84
	Br(3)– $\mu_3$ -F(4)	2.128(6)	2.15
	Br(3)– $\mu_2$ -F(7)	1.927(8)	1.93
	Br(3)–F(5, 6)	1.804(7), 1.767(6)	1.81, 1.77
$\text{BrF}_3$ -unit	Br(4)– $\mu_2$ -F(7)	2.391(8)	2.39
	Br(4)–F(8, 9, 10)	1.854(7), 1.711(6), 1.851(7)	1.83, 1.75, 1.83

ing fluorine atoms. All of these distances are in good agreement with the previously quantum-chemically calculated  $[\text{Br}_4\text{F}_{13}]^-$  anion,<sup>[26]</sup> whose bond lengths are also listed in Table 2. Also, the almost planar kite-like  $\text{BrF}_4$ -units, which were described for the  $[\text{Br}_3\text{F}_{10}]^-$  anion, are still present. This can be seen by considering the angle sum inside these kites with ca.  $360^\circ$ . The almost planar arrangement of F atoms around the Br(3) atom is of course no more kite-like, but better described as a trapezoid.

The other  $[\text{Br}_4\text{F}_{13}]^-$  anion, which shows some F atom disorder, is illustrated in Figure 4 together with the molecular structure of the quantum-chemically predicted anion shown in Scheme 2b.

To structurally describe the anion, we only use F(20A) which has a site occupancy factor of 0.67(9). If we consider the F(20B) atom, the anion becomes similar to the isomeric  $[\text{Br}_4\text{F}_{13}]^-$  anion described above. We now neglect F(20B) for simplicity. Therefore, the anion can be best described as a  $[\text{Br}_2\text{F}_7]^-$  unit carrying two additional  $\text{BrF}_3$  molecules, such as the quantum-chemically

predicted one in Scheme 2b. The  $[\text{Br}_2\text{F}_7]^-$  unit is built from the Br(6) and Br(7) atoms which are connected via the  $\mu_2$ -bridging F(20A) atom. The  $\mu_2$ -F(20A)–Br bond lengths are with 2.036(14) and 2.129(17) Å similar to the  $\mu_2$ -F–Br bond length in  $\text{Rb}[\text{Br}_2\text{F}_7]$  (2.145(2), 2.115(2) Å).<sup>[22]</sup> The other Br–F bond lengths are also quite similar to those in  $\text{Rb}[\text{Br}_2\text{F}_7]$  with 1.845(2)–1.890(2) Å for the  $F_{\text{cis}}$  atoms, and 1.767(2) and 1.780(2) Å for the  $F_{\text{trans}}$  atoms,<sup>[22]</sup> whereas the longest distances are those which are in *cis* position to the  $\mu_2$ -F(20A) atom. Two additional  $\text{BrF}_3$  molecules are attached to the  $[\text{Br}_2\text{F}_7]^-$  unit. However, none of the two is bound to the  $\mu_2$ -bridging F(20A) atom, as it was the case for the  $[\text{Br}_3\text{F}_{10}]^-$  anion.<sup>[22]</sup> They are connected to the F atoms F(17) and F(19), which both belong to the same  $[\text{BrF}_4]^-$  unit and are in the *cis* position to the  $\mu_2$ -F(20A) atom. Both  $\text{BrF}_3$  molecules have distances of more than 2.4 Å to the “ $\mu_2$ -F” atoms F(17) and F(19). As these distances are larger than in the above described  $[\text{Br}_4\text{F}_{13}]^-$  anion they are shown as dashed lines in Figure 4. The Br–F bonds in the  $\text{BrF}_3$  molecules are with

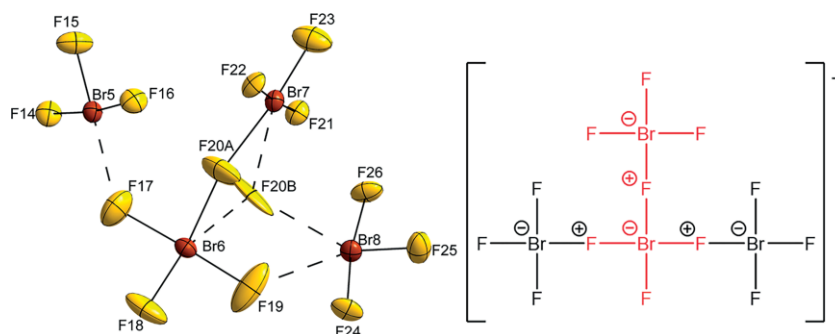


Figure 4. Left: the  $[\text{Br}_4\text{F}_{13}]^-$  anion which could be only refined with disordered fluorine atoms (F20A and F20B). Atom distances are given in Å. The longer distances to the additional  $\text{BrF}_3$  molecules are shown dashed. Displacement ellipsoids are shown at the 70 % probability level at 100 K. Right: structural formula of the  $[\text{Br}_4\text{F}_{13}]^-$  anion shown for direct comparison.

Table 3. Selected Br–F bond lengths (in Å) of the  $[\text{Br}_4\text{F}_{13}]^-$  anion shown in Figure 4.

		Single crystal X-ray diffraction at 100 K	DFT-PBE0/SVP calculation at 0 K
$\text{BrF}_3$ -units	Br(5)– $\mu_2$ -F(17)	2.408(9)	2.47
	Br(5)–F(14,15,16)	1.847(6), 1.714(7), 1.850(6)	1.85, 1.75, 1.86
	Br(8)– $\mu_2$ -F(19)	2.663(11)	2.39
	Br(8)–F(24,25,26)	1.833(7), 1.694(7), 1.841(6)	1.85, 1.76, 1.86
$\text{Br}_2\text{F}_7$ -unit	Br(6)– $\mu_2$ -F(17,19)	1.920(8), 1.822(9)	1.89, 1.93
	Br(6)–F(18)	1.758(7)	1.80
	Br(6)– $\mu_2$ -F(20A,B)	2.036(14), 2.06(3)	2.04
	Br(7)– $\mu_2$ -F(20A,B)	2.129(17), 2.31(6)	2.16
	Br(7)–F(21,22,23)	1.856(6), 1.865(6), 1.740(7)	1.87, 1.89, 1.78

1.833(7)–1.850(6) Å for the longer and 1.694(7) and 1.714(7) Å for the shorter bonds, only slightly different from those in free  $\text{BrF}_3$  (gas phase: 1.810 and 1.720 Å).<sup>[32]</sup> If a  $\text{BrF}_3$  molecule is bound to a fluoride anion forming any of the fluoridobromate(III) anions described above, all Br–F bonds would be significantly elongated compared to those of free  $\text{BrF}_3$  molecules. We therefore conclude that there is only a weak interaction between the  $\text{BrF}_3$  molecules and the  $[\text{Br}_2\text{F}_7]^-$  anion. If we also consider F(20B) and have a look at the elongated displacement ellipsoids of the atoms F(17–19), it is plausible that the complete  $[\text{BrF}_4]^-$  unit is slightly disordered. A comparison of observed and quantum-chemically predicted bond lengths is shown in Table 3.

Considering the two isomeric  $[\text{Br}_4\text{F}_{13}]^-$  anions described here, one may wonder, as to why their molecular structure is not chain-like as in Scheme 2a, or tetrahedron-like, that is, why not four  $\text{BrF}_3$  molecules coordinate to a central  $\mu_4\text{-F}^-$  anion. While the chain-like isomer shown in Scheme 2a turned out to be the most energetically stable in the quantum-chemical calculations for the gas phase, the order of stability may well change in the solid state, especially since the isomers were all close in energy.<sup>[26]</sup> Previously we had also calculated a tetrahedron-like species with a central  $\mu_4\text{-F}$  atom for the gas phase. It also turned out to be a true local minimum, however with the highest energy in comparison to others.<sup>[26]</sup>

In the crystal structure of the compound discussed here, the barium cations are surrounded by twelve fluorine atoms each in coordination polyhedra best described as distorted icosahedra. The Ba–F distances lie in the range from 2.741(7) to 3.087(6) Å and are similar to those described above for  $\text{Ba}[\text{Br}_3\text{F}_{10}]_2 \cdot \text{BrF}_3$  and also similar to those reported in the literature with for example 2.78(2)–3.06(2) Å in  $\text{Ba}[\text{AuF}_4]_2$ .<sup>[33]</sup> The icosahedra form close packed layers perpendicular to the *c* axis and the stacking of the layers corresponds to hexagonal close packing, that is, to the arrangement of Mg atoms in the Mg structure type. As the packing is not cubic close but hexagonally close, empty

channels of octahedral voids are present. The symmetry-independent  $[\text{Br}_4\text{F}_{13}]^-$  anions are located within the “empty” channels, that is, in the octahedral voids of the Mg structure type, while the  $[\text{Br}_3\text{F}_{10}]^-$  anions are located close to the faces of the tetrahedral voids. Overall, a three-dimensional infinite network structure is present. The crystal structure of  $\text{Ba}_2[\text{Br}_3\text{F}_{10}]_2[\text{Br}_4\text{F}_{13}]_2$  is shown in Figure 5.

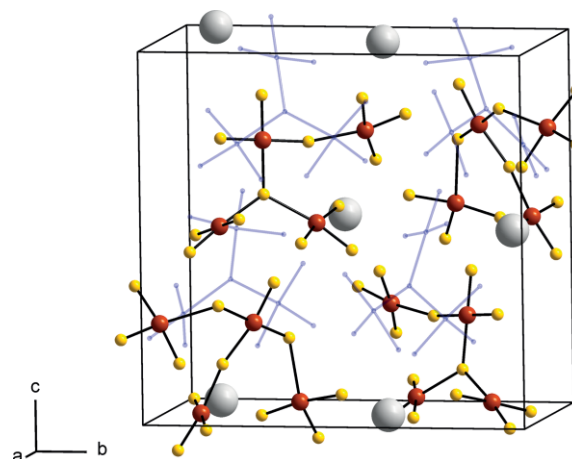


Figure 5. Crystal structure of  $\text{Ba}_2[\text{Br}_3\text{F}_{10}]_2[\text{Br}_4\text{F}_{13}]_2$ . The  $[\text{Br}_3\text{F}_{10}]^-$  anions are shown as blue wireframes for the sake of clarity.  $[\text{Br}_4\text{F}_{13}]^-$  anions are shown in ball and stick style. Br atoms in brown, F atoms in yellow, and Ba atoms in grey, all with arbitrary radii. Only one orientation of the disordered anions is shown.

### Quantum-Chemical Calculations

We carried out a structural optimization of the lattice parameters and atom positions for  $\text{Ba}_2[\text{Br}_3\text{F}_{10}]_2[\text{Br}_4\text{F}_{13}]_2$  at the DFT-PBE0/SVP level of theory using the CRYSTAL17 software.<sup>[34]</sup> In the quantum-chemical calculations, the site occupation factors of the F(20A) and F(20B) atoms were set to one and zero, re-

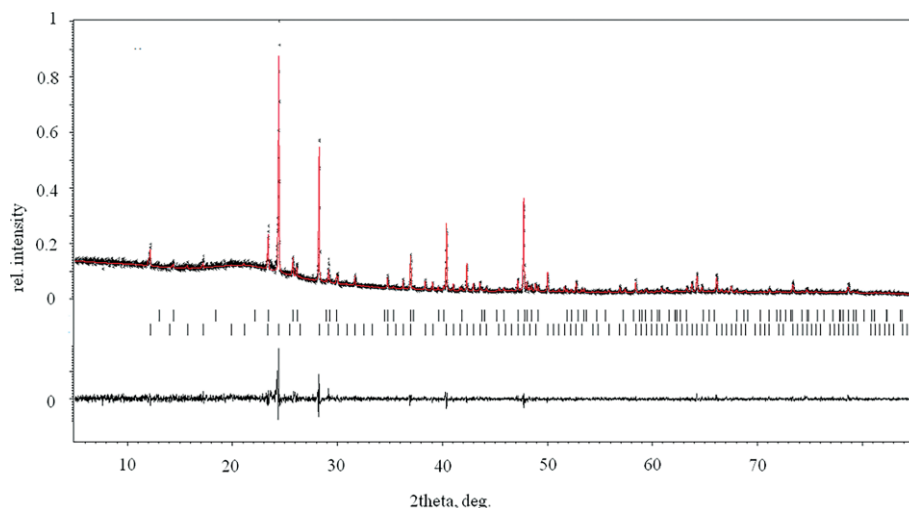


Figure 6. Rietveld refinement on the observed (black) and calculated (red) powder X-ray diffraction pattern of a sample that contains  $\text{Ba}[\text{Br}_3\text{F}_{10}]_2 \cdot \text{BrF}_3$  which was evacuated shortly. The calculated reflection positions are indicated by the vertical bars below the pattern (first row  $\text{Ba}[\text{Br}_4]_2$ , second row  $\text{Ba}[\text{Br}_3\text{F}_{10}]_2 \cdot \text{BrF}_3$ ). The curve at the bottom represents the difference between the observed and the calculated intensities.  $R_p = 6.18$ ,  $R_{wp} = 8.26$  (not background corrected R values),  $S = 1.19$ .

spectively. The optimization of the crystal structure led to calculated lattice parameters of  $a = 8.7856$ ,  $b = 15.0668$ ,  $c = 14.4029$  Å,  $\beta = 90.0484^\circ$ ,  $V = 1906.52$  Å<sup>3</sup>,  $Z = 2$ . The calculated atom positions agree well with the experimentally observed ones and are shown in Table S5. A comparison of Br–F bond lengths and F–Br–F angles is shown in Table S7. For the Br–F bonds the maximum difference between calculated and experimentally observed data is for the Br–F(19) distances with up to 10 %, which may be expected as the displacement ellipsoid of that F atom is quite elongated. All other Br–F bond lengths are within 4 % in a good accordance. The highest differences in the angles are also for the cases where F(19) is included (up to 10 % difference to the experimentally observed angles).

### Powder X-ray Diffraction

A sample containing Ba[Br<sub>3</sub>F<sub>10</sub>]<sub>2</sub>·BrF<sub>3</sub> in BrF<sub>3</sub> was only shortly exposed to a vacuum at room temperature to prevent its complete decomposition to Ba[BrF<sub>4</sub>]<sub>2</sub>. The obtained powder was transferred into a glovebox and a part of the sample was ground using an agate mortar and filled into a silica capillary. A powder X-ray pattern was recorded after flame-sealing the silica capillary under inert gas. The Rietveld refinement on the powder X-ray pattern (Figure 6) showed the presence of 83(2) % Ba[Br<sub>3</sub>F<sub>10</sub>]<sub>2</sub>·BrF<sub>3</sub> and 17 % Ba[BrF<sub>4</sub>]<sub>2</sub> as crystalline phases. Details of the Rietveld refinement are available from Table S8.

It is not clear if Ba[BrF<sub>4</sub>]<sub>2</sub> was formed by the careful evacuation process to remove the solvent BrF<sub>3</sub>, or if it was already present in the form of very small crystals. The presence of Ba<sub>2</sub>[Br<sub>3</sub>F<sub>10</sub>]<sub>2</sub>[Br<sub>4</sub>F<sub>13</sub>]<sub>2</sub> was not to be expected as it is only obtained by cooling the sample, which was not the case here. Ba[BrF<sub>4</sub>]<sub>2</sub> is the decomposition product of Ba[Br<sub>3</sub>F<sub>10</sub>]<sub>2</sub>·BrF<sub>3</sub> under vacuum, which we showed in an experiment where a sample was placed under vacuum at room temperature until the pressure no longer changed (see powder X-ray diffraction pattern and IR spectrum in Figure S1 and S2).

### Vibrational Spectroscopy

An IR spectrum was recorded on the same sample as the powder X-ray pattern and thus contained the above stated amounts of Ba[Br<sub>3</sub>F<sub>10</sub>]<sub>2</sub>·BrF<sub>3</sub> and Ba[BrF<sub>4</sub>]<sub>2</sub>. The ATR-IR spectrum (Figure 7) shows three strong and broad bands at 636, 506 and 426 cm<sup>-1</sup> (in black). Bands of Ba[BrF<sub>4</sub>]<sub>2</sub> were reported to occur at 546, 485, and 416 cm<sup>-1</sup>,<sup>[20]</sup> and strong bands of BrF<sub>3</sub> at 682 and 668, around 614, and at 242 cm<sup>-1</sup>.<sup>[54]</sup> The IR spectrum of Cs[Br<sub>3</sub>F<sub>10</sub>]<sup>[22]</sup> is shown in red for comparison. Three strong bands (with shoulders) are present, which are only shifted slightly compared to the bands observed here. Because of the slight similarity we assume the presence of [Br<sub>3</sub>F<sub>10</sub>]<sup>-</sup> anions besides [BrF<sub>4</sub>]<sup>-</sup> anions. We also calculated the IR spectrum for Ba<sub>2</sub>[Br<sub>3</sub>F<sub>10</sub>]<sub>2</sub>[Br<sub>4</sub>F<sub>13</sub>]<sub>2</sub>, which is added to Figure 4 in blue. Compared with the recorded spectrum in black, some bands, especially the band at around 570 cm<sup>-1</sup>, are only present in the calculated spectrum. The main contribution to this band arises from Br–F stretching vibrations within both [Br<sub>4</sub>F<sub>13</sub>]<sup>-</sup> anions (mainly stretching vibrations of the atoms F11, F13 and F24, F26). This indicates that [Br<sub>4</sub>F<sub>13</sub>]<sup>-</sup> anions are not present in the sample at room temperature, as may have been expected. Due to the disordered and underoccupied BrF<sub>3</sub> molecules of crystallization in Ba[Br<sub>3</sub>F<sub>10</sub>]<sub>2</sub>·BrF<sub>3</sub>, we could not quantum-chemically calculate its IR spectrum.

We carried out Raman spectroscopic measurements on crystals submerged in liquid BrF<sub>3</sub> inside a FEP tube. The experimentally obtained spectrum of Ba[Br<sub>3</sub>F<sub>10</sub>]<sub>2</sub>·BrF<sub>3</sub> and the calculated spectrum for Ba<sub>2</sub>[Br<sub>3</sub>F<sub>10</sub>]<sub>2</sub>[Br<sub>4</sub>F<sub>13</sub>]<sub>2</sub> are shown in Figure 8.

For Ba[BrF<sub>4</sub>]<sub>2</sub>, bands at 549, 491, 450, 273, and 195 cm<sup>-1</sup> and for BrF<sub>3</sub> strong bands at 675 and 552 cm<sup>-1</sup> were reported,<sup>[20,54]</sup> thus some overlap is expected. In the recorded spectrum, three strong bands at 671 (with shoulders), at 535 and at 520 cm<sup>-1</sup> are present. These three strong bands overlap with bands in the calculated spectrum of Ba<sub>2</sub>[Br<sub>3</sub>F<sub>10</sub>]<sub>2</sub>[Br<sub>4</sub>F<sub>13</sub>]<sub>2</sub>. In the calculated spectrum, these bands arise from Br–F<sub>trans</sub> stretching vibrations of both the [Br<sub>3</sub>F<sub>10</sub>]<sup>-</sup> and [Br<sub>4</sub>F<sub>13</sub>]<sup>-</sup> anions. However, the bands

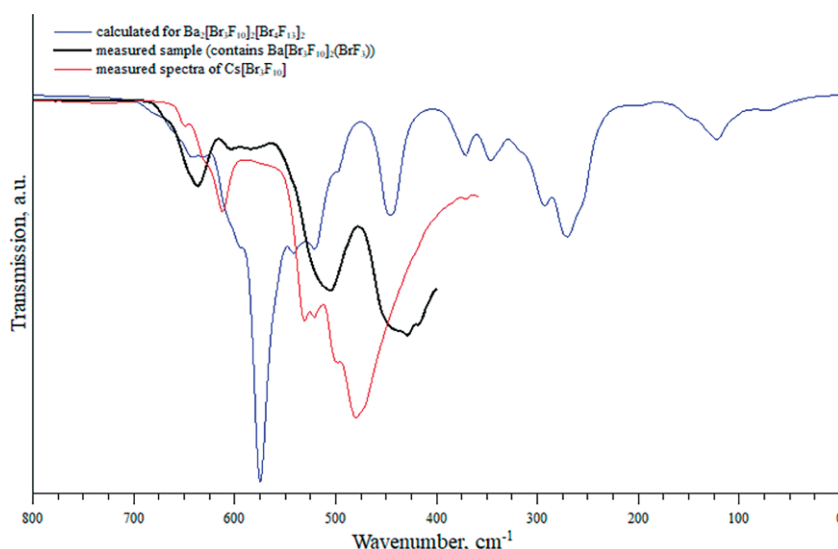


Figure 7. ATR-IR spectrum of Ba[Br<sub>3</sub>F<sub>10</sub>]<sub>2</sub>·BrF<sub>3</sub> in black, the calculated spectrum of Ba<sub>2</sub>[Br<sub>3</sub>F<sub>10</sub>]<sub>2</sub>[Br<sub>4</sub>F<sub>13</sub>]<sub>2</sub> in blue (DFT-PBE0/SVP level of theory), and for comparison the spectrum of Cs[Br<sub>3</sub>F<sub>10</sub>]<sup>[22]</sup> in red. The sample contains ca. 17 % of Ba[BrF<sub>4</sub>]<sub>2</sub>.

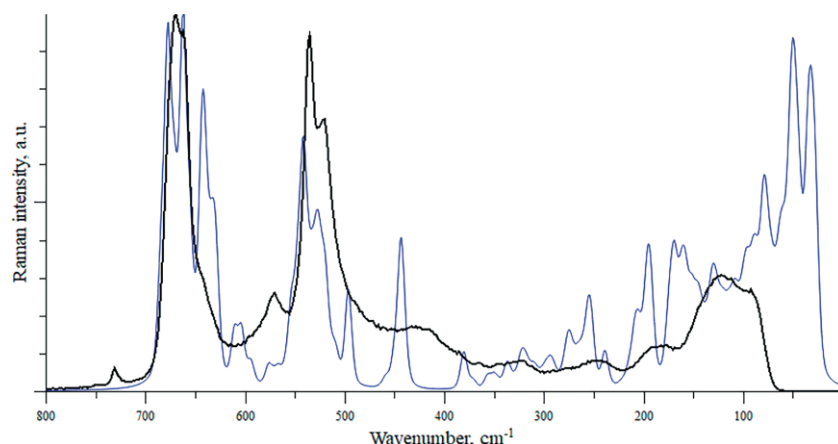


Figure 8. Raman spectrum of  $\text{Ba}[\text{Br}_3\text{F}_{10}]_2\cdot\text{BrF}_3$  (black) and the calculated spectrum of  $\text{Ba}_2[\text{Br}_3\text{F}_{10}]_2[\text{Br}_4\text{F}_{13}]_2$  (blue, DFT-PBE0/SVP level of theory).

at about 640 and 440  $\text{cm}^{-1}$ , not present in the experimental spectrum, clearly arise from the  $[\text{Br}_4\text{F}_{13}]^-$  anion as evidenced by the quantum-chemical calculations where the band at 640  $\text{cm}^{-1}$  is due to  $\text{Br}-\text{F}_{\text{trans}}$  and the one at 440  $\text{cm}^{-1}$  is due to both  $\mu_3$  and  $\mu_2$   $\text{Br}-\mu-\text{F}$  vibrations.

## Conclusion

We synthesized two new fluoridotetrabromate(III) anions, which were predicted previously by quantum-chemical calculations by reacting  $\text{BrF}_3$  with  $\text{BaF}_2$  or  $\text{BaCl}_2$ . Crystal selection at room temperature results in crystals of the composition  $\text{Ba}[\text{Br}_3\text{F}_{10}]_2\cdot\text{BrF}_3$ , where disordered  $\text{BrF}_3$  molecules of crystallization are present, while selection at slightly lower temperature gives crystals of the composition  $\text{Ba}_2[\text{Br}_3\text{F}_{10}]_2[\text{Br}_4\text{F}_{13}]_2$ . Two structurally different  $[\text{Br}_4\text{F}_{13}]^-$  anions are present, one is better described as a  $[\text{Br}_2\text{F}_7]^-$  anion with two  $\text{BrF}_3$  molecules loosely bound, while the other  $[\text{Br}_4\text{F}_{13}]^-$  anion is best described as a  $[\text{Br}_3\text{F}_{10}]^-$  anion where an additional  $\text{BrF}_3$  molecule is more tightly bound. Powder X-ray diffraction measurements at room temperature showed the bulk phase to mainly consist of  $\text{Ba}[\text{Br}_3\text{F}_{10}]_2\cdot\text{BrF}_3$ . The compound is not stable under vacuum and decomposes to  $\text{Ba}[\text{BrF}_4]_2$ .

## Experimental Section

$\text{F}_2$ ,  $\text{BrF}_3$ , and compounds containing fluoridobromate(III) anions are powerful oxidants and may pose a working hazard to those being unexperienced, untrained, and unskilled. Suitable protective gear should be worn at all times and access to proper medical treatment is necessary.

**Synthesis of  $\text{BrF}_3$ :**  $\text{BrF}_3$  was synthesized by passing fluorine (Solvay, > 99.0 %) through bromine (Merck, p. A.). The reaction was carried out in a FEP (perfluorinated ethylene-propylene) U-tube which was cooled with ice from the outside. After the synthesis, the remaining bromine was pumped-off and the  $\text{BrF}_3$  was stored in previously passivated FEP tubes.

**Synthesis of  $\text{Ba}[\text{Br}_3\text{F}_{10}]_2\cdot\text{BrF}_3$ :** In a first experiment a previously passivated PFA tube was loaded with 0.10 g (0.57 mmol)  $\text{BaCl}_2$  and an excess of  $\text{BrF}_3$  was added dropwise using a PFA pipette. The formed suspension was heated up to 120 °C using a heat gun and cooled down to ambient temperature. During this process colorless

crystals precipitated, from which four were selected for single-crystal X-ray diffraction measurements. After the measurement, the remaining solvent was evaporated and neat  $\text{Ba}[\text{BrF}_4]_2$ , identified using powder X-ray diffraction (Figure S1) and IR spectroscopy (Figure S2), could be obtained.

**Synthesis of  $\text{Ba}_2[\text{Br}_3\text{F}_{10}]_2[\text{Br}_4\text{F}_{13}]_2$ :** The second experiment was done similar to the first one. Instead of  $\text{BaCl}_2$  we used  $\text{BaF}_2$  (32.0 mg, 0.18 mmol), a smaller amount of  $\text{BrF}_3$  (151.3 mg, 1.11 mmol) and the temperature was only 100 °C. This time the formed crystals were selected by cooling down the perfluorinated oil to a temperature which was close to the melting point of  $\text{BrF}_3$  (ca. 10 °C). The crystals were placed in the oil and some crystals were selected for X-ray diffraction analysis using a visible-light microscope. After the X-ray diffraction measurement, we pumped off only the solvent (room temperature), and brought the remaining crystals inside the glove box (argon 5.0 (Praxair) atmosphere). From this sample a powder X-ray diffraction pattern and an IR spectrum were measured.

**Powder X-ray diffraction:** The powder X-ray diffraction patterns were recorded at ambient temperature with a STOE Stadi MP powder diffractometer in Debye–Scherrer geometry (capillary) or transmission geometry (flat sample). The diffractometer was operated with  $\text{Cu}-K_{\alpha 1}$  radiation (1.5406 Å, Ge(111) monochromator) and equipped with a Mythen1K detector. One sample ( $\text{Ba}[\text{Br}_3\text{F}_{10}]_2\cdot\text{BrF}_3$ ) was measured in a sealed 0.5 mm fused silica capillary (WJM Glas) and the  $\text{Ba}[\text{BrF}_4]_2$  sample was measured between two pieces of a tape (3MScotch® Magic™). Both sample preparations were carried out in a glove box under argon (5.0, Praxair) atmosphere. The evaluation of the powder X-ray patterns were carried out with the WinXPOW 3.07 software package.<sup>[35]</sup> The Rietveld refinement was performed with Jana2006.<sup>[36]</sup>

### Single crystal X-ray diffraction

The crystals were selected under perfluorinated oil (Galden HT 270) and mounted using a MiTeGen loop. To select some crystals at lower temperatures the oil was cooled with liquid nitrogen until some drops of  $\text{BrF}_3$  solidified. The glass microscope slide was placed over a Dewar vessel with liquid nitrogen to cool it from below and a precooled stream of nitrogen was passed over the sample holder to prevent contact with air and ice formation. After the  $\text{BrF}_3$  liquefied, the sample was transferred inside the oil, whereas the estimated temperature of the oil was only slightly above the melting point of  $\text{BrF}_3$ . Intensity data of suitable crystals were recorded with an IPDS 2 diffractometer (Stoe & Cie) where the crystals were kept

under a stream of nitrogen. The diffractometer was operated with Mo- $K_{\alpha}$  radiation (0.71073 Å, graphite monochromator) and equipped with an image plate detector. Evaluation, integration and reduction of the diffraction data were carried out using the Stoe X-Area software suite.<sup>[37]</sup> The numerical absorption corrections were applied with the modules X-Shape and X-Red32 of the X-Area software suite. The structures were solved with dual-space methods (SHELXT-2014/5)<sup>[38]</sup> and refined against  $F^2$  (SHELXL-2018/3).<sup>[39]</sup> The squeeze procedure was used on Ba[Br<sub>3</sub>F<sub>10</sub>]·BrF<sub>3</sub>. Representations of the crystal-structures were created with the Diamond software.<sup>[40]</sup>

Deposition Numbers 2019331 and 2019332 contain the supplementary crystallographic data for this paper. These data are provided free of charge by the joint Cambridge Crystallographic Data Centre and Fachinformationszentrum Karlsruhe Access Structures service [www.ccdc.cam.ac.uk/structures](http://www.ccdc.cam.ac.uk/structures).

**IR spectroscopy:** Infrared spectra were measured on a Bruker Alpha Platinum FT-IR spectrometer using the ATR Diamond module with a resolution of 4 cm<sup>-1</sup>. The spectrometer was located inside a glovebox under argon (5.0, Praxair) atmosphere. For data collection, the OPUS 7.2 software was used.<sup>[41]</sup>

**Raman spectroscopy:** The Raman spectrum was collected by using a Labram HR800 (JobinYvon) instrument equipped with a 25 mW He/Ne laser tube ( $\lambda = 623.817$  nm). The collected data were handled with the LabSpec software package.<sup>[42]</sup> The sample was prepared freshly before measuring the Raman spectra by placing BaF<sub>2</sub> (72.9 mg, 0.42 mmol) in a 1/8" FEP tube and adding BrF<sub>3</sub> (136 mg, 0.99 mmol). After the suspension was heated up to 120 °C, we let it cool down to room temperature and sealed the FEP tube.

**Thermal decomposition:** The thermal measurement was done on a DSC-TGA 3 (Mettler Toledo) with a heating rate of 10 °C/min under a stream of nitrogen (30 mL/min). Data were collected with the STARe Software package.<sup>[43]</sup>

**Quantum-chemical calculations:** The solid-state quantum-chemical calculations were carried out with the CRYSTAL17 program package.<sup>[34]</sup> PBE0 hybrid density functional method and Gaussian-type basis sets of split-valence + polarization quality were used.<sup>[44]</sup> The basis sets for F, Br, and Ba have been previously derived from the molecular Karlsruhe def2 basis sets.<sup>[20,31,45,46]</sup> The reciprocal space was sampled using a 2×1×1 Monkhorst-Pack-type  $k$ -point grid.<sup>[47]</sup> For the evaluation of the Coulomb and exchange integrals (TOLINTEG), tight tolerance factors of 8, 8, 8, 8, and 16 were used. Both the atomic positions and lattice constants were fully optimized within the constraints imposed by the space group symmetry. Harmonic vibrational frequencies at the  $\Gamma$ -point were calculated numerically with the central differences scheme implemented in CRYSTAL.<sup>[48,49]</sup> IR and Raman intensities were obtained with the Coupled Perturbed Kohn–Sham method implemented in CRYSTAL.<sup>[50–52]</sup> IR spectrum was broadened using Lorentzian peak profile and FWHM of 16 cm<sup>-1</sup>. Raman spectrum was broadened using pseudo-Voigt peak profile (50:50 Lorentzian:Gaussian) and FWHM of 8 cm<sup>-1</sup>. Room temperature and laser wavelength of 532 nm were used for simulating the Raman spectrum. The vibrational spectra were interpreted by visual inspection of the normal modes using the J mol program.<sup>[53]</sup>

## Acknowledgments

We want to thank the Deutsche Forschungsgemeinschaft for funding, the X-ray facilities for their services and Benjamin Scheibe and H. Lars Deubner for Raman measurements. Furthermore, we want to thank Solvay for kind donations of F<sub>2</sub>. A. J. K.

acknowledges computational resources provided by CSC, the Finnish IT Center for Science. Open access funding enabled and organized by Projekt DEAL.

**Keywords:** Fluoridobromate(III) · Fluorides · Bromine trifluoride · Structure elucidation · Quantum-chemical calculations

- [1] A. G. Sharpe, H. J. Emeléus, *J. Chem. Soc.* **1948**, 0, 2135–2138.
- [2] S. I. Ivlev, R. V. Ostvald, F. Kraus, *Monatsh. Chem.* **2016**, 147, 1661–1668.
- [3] A. I. Popov, Yu. M. Kiselev, V. F. Sukhoverkhov, N. A. Chumaevsky, O. A. Krasnyanskaya, A. T. Sadikova, *Russ. J. Inorg. Chem.* **1987**, 32, 619–622.
- [4] A. I. Popov, Yu. M. Kiselev, V. F. Sukhoverkhov, N. A. Chumaevsky, O. A. Krasnyanskaya, A. T. Sadikova, *Zh. Neorg. Khim.* **1987**, 32, 1007–1012.
- [5] S. Siegel, *Acta Crystallogr.* **1956**, 9, 493–495.
- [6] S. Siegel, *Acta Crystallogr.* **1957**, 10, 380–380.
- [7] W. G. Sly, R. E. Marsh, *Acta Crystallogr.* **1957**, 10, 378–379.
- [8] A. Chrétien, P. Bouy, *C. R. Hebd. Seances Acad. Sci.* **1958**, 246, 2493–2495.
- [9] A. J. Edwards, G. R. Jones, *J. Chem. Soc. A* **1969**, 1936–1938.
- [10] K. O. Christe, C. J. Schack, *Inorg. Chem.* **1970**, 9, 1852–1858.
- [11] I. Sheft, A. F. Martin, J. J. Katz, *J. Am. Chem. Soc.* **1956**, 78, 1557–1559.
- [12] S. I. Ivlev, A. J. Karttunen, R. Ostvald, F. Kraus, *Z. Anorg. Allg. Chem.* **2015**, 641, 2593–2598.
- [13] A. R. Mahjoub, A. Hoser, J. Fuchs, K. Seppelt, *Angew. Chem. Int. Ed.* **1989**, 28, 000–000; *Angew. Chem.* **1989**, 101, 1528–1529.
- [14] A. R. Mahjoub, A. Hoser, J. Fuchs, K. Seppelt, *Angew. Chem. Int. Ed. Engl.* **1989**, 28, 1526–1527; *Angew. Chem.* **1989**, 101, 1528.
- [15] S. Ivlev, P. Woidy, V. Sobolev, I. Gerin, R. Ostvald, F. Kraus, *Z. Anorg. Allg. Chem.* **2013**, 639, 2846–2850.
- [16] V. F. Sukhoverkhov, N. D. Takanova, A. A. Uskova, *Zh. Neorg. Khim.* **1976**, 21, 2245–2249.
- [17] V. F. Sukhoverkhov, Ya. Moltashova, *Zh. Neorg. Khim.* **1980**, 25, 3041–3045.
- [18] K. O. Christe, W. W. Wilson, *Inorg. Chem.* **1986**, 25, 1904–1906.
- [19] W. W. Wilson, K. O. Christe, *Inorg. Chem.* **1989**, 28, 4172–4175.
- [20] S. Ivlev, V. Sobolev, M. Hoelzel, A. J. Karttunen, T. Müller, I. Gerin, R. Ostvald, F. Kraus, *Eur. J. Inorg. Chem.* **2014**, 2014, 6261–6267.
- [21] L. Stein, *J. Fluorine Chem.* **1985**, 27, 249–256.
- [22] S. I. Ivlev, A. J. Karttunen, R. V. Ostvald, F. Kraus, *Chem. Commun.* **2016**, 52, 12040–12043.
- [23] S. I. Ivlev, P. Woidy, I. I. Zherin, R. V. Ostvald, F. Kraus, M. Yu. Voytenko, V. V. Shagalov, *Procedia Chem.* **2014**, 11, 35–42.
- [24] J. Bandemehr, M. Sachs, S. I. Ivlev, A. J. Karttunen, F. Kraus, *Eur. J. Inorg. Chem.* **2020**, 2020, 64–70.
- [25] R. Schmidt, B. G. Müller, *Z. Anorg. Allg. Chem.* **2004**, 630, 2393–2397.
- [26] J. Linnera, S. I. Ivlev, F. Kraus, A. J. Karttunen, *Z. Anorg. Allg. Chem.* **2019**, 645, 284–291.
- [27] A. L. Spek, *Acta Crystallogr., Sect. C: Struct. Chem.* **2015**, 71, 9–18.
- [28] A. M. Ellern, M. Yu. Antipin, Yu. T. Struchkov, V. F. Sukhoverkhov, *Russ. J. Inorg. Chem.* **1991**, 36, 792–794.
- [29] T. Bunic, M. Tramsek, E. Goresnik, B. Zemva, *Solid State Sci.* **2006**, 8, 927–931.
- [30] O. Ruff, A. Braid, O. Bretschneider, W. Menzel, H. Plaut, *Z. Anorg. Allg. Chem.* **1932**, 206, 59–64.
- [31] F. Weigend, R. Ahlrichs, *Phys. Chem. Chem. Phys.* **2005**, 7, 3297–3305.
- [32] D. W. Magnuson, *J. Chem. Phys.* **1957**, 27, 223–226.
- [33] B. G. Müller, *Z. Anorg. Allg. Chem.* **1987**, 555, 57–63.
- [34] R. Dovesi, A. Erba, R. Orlando, C. M. Zicovich-Wilson, B. Civalleri, L. Maschio, M. Rérat, S. Casassa, J. Baima, S. Salustro, B. Kirtman, *Wiley Interdiscip. Rev. : Comput. Mol. Sci.* **2018**, e1360.
- [35] STOE WinXPow, STOE & Cie GmbH, Darmstadt, Germany, **2015**.
- [36] V. Petříček, M. Dušek, L. Palatinus, *Z. Kristallogr.* **2014**, 229, 345–352.
- [37] X-Area, STOE & Cie GmbH, Darmstadt, Germany, **2018**.
- [38] G. M. Sheldrick, *Acta Crystallogr., Sect. A: Found. Adv.* **2015**, 71, 3–8.
- [39] G. M. Sheldrick, *Acta Crystallogr., Sect. C: Struct. Chem.* **2015**, 71, 3–8.
- [40] K. Brandenburg, H. Putz, *Diamond - Crystal and Molecular Structure Visualization*, Crystal Impact GbR, Bonn, **2019**.
- [41] OPUS V7.2, Bruker Optik GmbH, Ettlingen, Germany, **2012**.

- [42] *LabSpec Spectroscopy Suit Software*, HORIBA Scientific, **2000**.
- [43] *STARe V14.00*, Mettler-Toledo GmbH, Analytical, Schwerzenbach, Switzerland, **2016**.
- [44] C. Adamo, V. Barone, *J. Chem. Phys.* **1999**, *110*, 6158–6170.
- [45] A. J. Karttunen, T. Tynell, M. Karppinen, *J. Phys. Chem. C* **2015**, *119*, 13105–13114.
- [46] S. I. Ivlev, M. R. Buchner, A. J. Karttunen, F. Kraus, *J. Fluorine Chem.* **2018**, *215*, 17–24.
- [47] H. J. Monkhorst, J. D. Pack, *Phys. Rev. B* **1976**, *13*, 5188–5192.
- [48] F. Pascale, C. M. Zicovich-Wilson, F. López Gejo, B. Cvalleri, R. Orlando, R. Dovesi, *J. Comput. Chem.* **2004**, *25*, 888–897.
- [49] C. M. Zicovich-Wilson, F. Pascale, C. Roetti, V. R. Saunders, R. Orlando, R. Dovesi, *J. Comput. Chem.* **2004**, *25*, 1873–1881.
- [50] L. Maschio, B. Kirtman, R. Orlando, M. Rérat, *J. Chem. Phys.* **2012**, *137*, 204113.
- [51] L. Maschio, B. Kirtman, M. Rérat, R. Orlando, R. Dovesi, *J. Chem. Phys.* **2013**, *139*, 164101.
- [52] L. Maschio, B. Kirtman, M. Rérat, R. Orlando, R. Dovesi, *J. Chem. Phys.* **2013**, *139*, 164102.
- [53] J mol: An Open-Source Java Viewer for Chemical Structures in 3D. <http://www.jmol.org/>, J mol Team, **2019**.
- [54] H. Selig, H. H. Claassen, J. H. Holoway, *J. Chem. Phys.* **1970**, *52*, 3517–3521.

---

Received: September 16, 2020